TOPICAL REVIEW • OPEN ACCESS

Transmission x-ray microscopy and its applications in battery material research—a short review

To cite this article: Stephanie Spence *et al* 2021 *Nanotechnology* **32** 442003

OPEN ACCESS
IOP Publishing
Nanotechnology

Nanotechnology **32** (2021) 442003 (10pp)
https://doi.org/10.1088/1361-6528/ac17ff

Topical Review

Transmission x-ray microscopy and its applications in battery material research—a short review

Stephanie Spence[1], **Wah-Keat Lee**[2], **Feng Lin**[1,*] **and Xianghui Xiao**[2,*]

[1] Department of Chemistry, Virginia Tech, Blacksburg, VA 24061, United States of America
[2] National Synchrotron Light Source II, Brookhaven National Laboratory, Upton, NY 11973, United States of America

E-mail: fenglin@vt.edu and xiao@bnl.gov

Received 15 January 2021, revised 17 May 2021
Accepted for publication 26 July 2021
Published 13 August 2021

Abstract

Transmission x-ray microscopy (TXM), which can provide morphological and chemical structural information inside of battery component materials at tens of nanometer scale, has become a powerful tool in battery research. This article presents a short review of the TXM, including its instrumentation, battery research applications, and the practical sample preparation and data analysis in the TXM applications. A brief discussion on the challenges and opportunities in the TXM applications is presented at the end.

Keywords: battery, cathode materials, transmission x-ray microscopy, synchrotron, XANES

(Some figures may appear in colour only in the online journal)

1. Introduction of transmission x-ray microscopy (TXM)

In studying complex systems composed of hierarchical structures, the system's performances are dependent on the structures and properties at all lengths of scales, from atomic to microscopic and macroscopic levels. Various microscopy techniques can be utilized to reveal the structures and properties at different lengths of scales. Compared to microscopy techniques based on other types of probing particles, e.g. electrons and infrared/visible light photons, x-rays have the advantage of high penetration power and are capable of looking at internal structures in bulk materials. Furthermore, x-ray techniques with a large field of view (FOV) that can measure a relatively large volume can mitigate the risk of biased, statistically irrelevant conclusions from other nano-resolution techniques that only measure very small volumes, usually near the surface. This is crucial in studying complex systems like batteries that have multiple components with hierarchical structures.

TXM techniques have been widely used in studying these complex systems [1–4]. TXM measures the transmitted x-rays after passage through the sample. x-rays interact with electrons in the matter when passing through a sample. X-rays can be scattered, absorbed, and re-emitted by electrons. The intensity, energy, and directions of the transmitted x-rays carry the sample information.

There are two general types of TXM techniques, full-field TXM and scanning TXM (STXM) [5, 6]. TXM and STXM are complementary in capabilities. Especially in the x-ray energy regime over transition metals' L-edges and O K-edge, STXM is typically employed in material science applications. This review focuses mainly on TXM applications in battery research. The readers who are interested in

* Authors to whom any correspondence should be addressed.

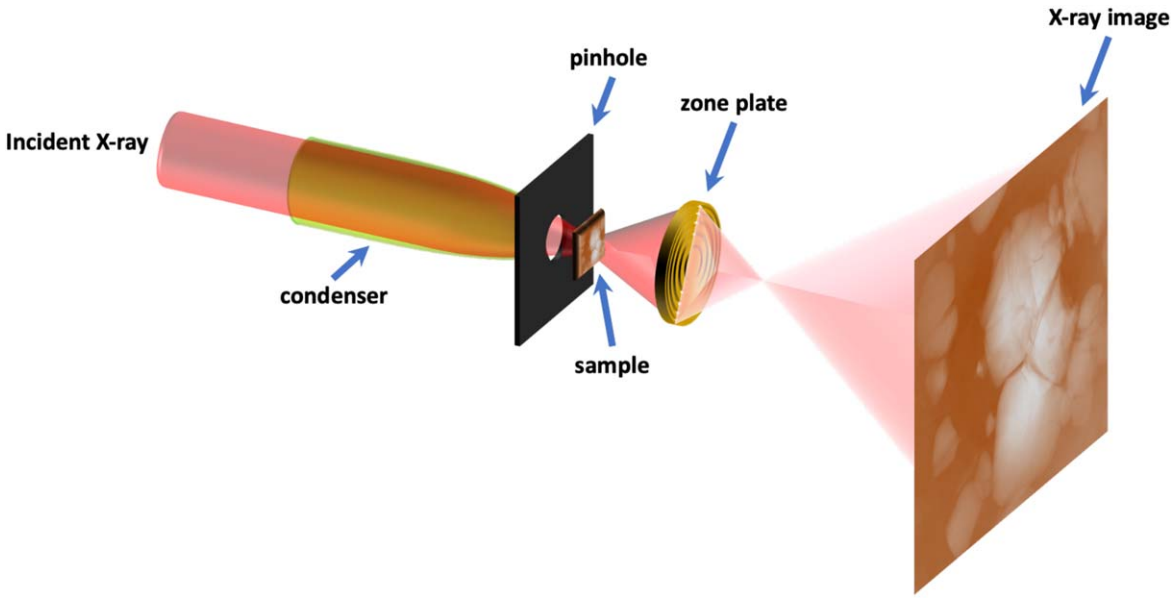

Figure 1. Schematic structure of TXM. Sample's x-ray images are recorded by an x-ray imaging detector (not shown).

Table 1. TXM operation chart at FXI beamline of NSLS-II.

	Spatial resolution	Temporal resolution	Operation energy range
2D XANES	30–50 nm	5–10 min scan^{-1}	5–15 keV
3D XANES	30–50 nm	~60 min scan^{-1}	
Tomography	30–50 nm	~15 s scan^{-1}	

STXM techniques can find the details in [6–8] and references therein.

Figure 1 presents the sketch of a TXM. TXM is analogous to conventional bright-field optical microscopes. A TXM is composed of an x-ray condenser, which is typically a shaped glass capillary or a grating-based beam shaper, an x-ray objective lens made of Fresnel zone plate (FZP) [9–11], and an x-ray detector composed of an x-ray scintillator, optical microscope objective lens, and an optical two-dimensional image detector. An FZP has concentric zone structures that alter the transmitted x-ray wave's optical path by half a wavelength through each zone. In the TXM setup, a sample is placed in between the condenser and the FZP lens. The sample's x-ray transmission image is magnified by the FZP lens and projected to the x-ray detector's scintillator. The scintillator converts x-ray photons into visible light photons that are further magnified by the optical microscope objective lens and registered in the image detector.

Since x-rays have wavelengths on the Angstrom scale, TXM can achieve high spatial resolutions within a few to tens of nanometer scales [6]. The FOV and resolution of the TXM depends on the illumination properties of the condenser, the zone plate objective and the visible light optics and detector. The typical FOV and spatial resolution with a TXM vary in ranges of tens to more than a hundred micrometers and 10–100 nm, respectively.

The TXM and STXM can operate in x-ray absorption spectroscopy (XAS) mode [6]. This is achieved by scanning the same sample at different energy points across one component element's x-ray absorption edge. When the incident x-ray photon energy is in the vicinity of the element's core electron binding energies, the interaction between x-ray photons and the core electrons is largely increased. The sample's absorption to the illuminating x-ray beam changes accordingly as a function of the x-ray photon energy. The x-ray energy dependent absorption spectrum carries the information of the sample's local structure configuration and chemical state. The XAS mode of TXM and STXM usually focus on the x-ray near-edge absorption spectroscopy (XANES) regime that presents the chemical state information of the measured samples. Generally speaking, one can understand TXM-XAS as performing XAS with a high spatial resolution.

An x-ray source is critical to TXM performances. The required number of photons is inversely proportional to the third to fourth power of the targeted spatial resolution [12, 13]. Therefore, a high intensity source is needed to obtain high-quality microscopy/spectroscopy data at high spatial resolution in a reasonable measurement time. Although lab-based TXMs exist, the performance of synchrotron-based TXMs are significantly better due to the superior synchrotron beam properties. As an example, the TXM at the National Synchrotron Light Source II at Brookhaven National Laboratory provides high-speed data acquisition at high spatial resolution (<30 nm) [14]. Table 1 summarizes the key performance parameters of this microscope. With the high

spatial and temporal resolution of this TXM, it is capable of revealing the structure evolution information in dynamic processes, e.g. morphological cracking behaviors and transition metal oxidation states in electrode particles under operating conditions. It provides high-throughput measurement capabilities that are crucial to obtain statistical information from microscopy experiments.

One of the most exciting developments of the TXM technique is the direct visualization and quantification of redox events in battery materials. Battery electrode particles represent a highly heterogeneous system where it can be very challenging for other high spatial resolution techniques to measure a sufficiently large volume that is statistically representative at the mesoscale. TXM, equipped with high-throughput capabilities, can not only provide a relatively good spatial resolution but also offer statistically significant results. In the next section, we will discuss some recent studies in applying TXM for understanding redox properties in intercalation cathodes. In this review, we will also provide some perspectives on data processing. However, the more extensive discussion will be reported elsewhere.

2. TXM applications in lithium-ion battery research

Since commercialization in the 1990s, the development of lithium-ion batteries has continued to advance both at the device level and electrode level [15]. Deeper understandings of the electrochemical reactions that occur in electrode materials have led to improvements in materials designs. Much of this understanding has been enabled by the use of synchrotron x-ray analytical techniques to study battery systems, which have matured in tandem with battery materials research. High-energy synchrotron x-ray techniques have become extremely important in the field of battery research as they allow scientists to study battery materials at multiple length scales, ranging from the battery system level at the macroscopic scale, to the electrode materials at the mesoscopic scale, down to the electronic structures of materials at the microscopic scale [1]. Synchrotron techniques allow for the study of battery materials under equilibrium conditions with *ex situ* experiments or during operation conditions with rapid *in situ* or *operando* studies [16]. Of the common techniques utilized, x-ray imaging techniques including tomography and STXM/TXM allow for the direct, nondestructive visualization of battery materials [16–22].

The chemical compositions and local valance states of elements in materials can be detected by combining TXM or STXM with XAS. Through probing the absorption edge of a specific element using the appropriate x-ray energy, researchers can visualize the distribution of different chemical species or monitor specific elements as they undergo oxidation and reduction in materials at the nanoscale (~30 nm) and in multiple dimensions [16, 23]. Synchrotron x-ray imaging techniques combine spectroscopy and microscopy to obtain data with both energy and space dimensions, providing researchers with extraordinary capabilities to see and study the three-dimensional chemical and morphological information in battery materials. Herein, we summarize recent developments in the field of lithium-ion battery research, which utilize TXM and STXM techniques to aid in answering fundamental questions about battery chemistries, including materials' structures, chemical or charge distributions, mechanisms and dynamics of Li^+ transportation, and chemomechanical degradation.

TXM has been used to determine elemental distributions and morphology in pristine layered oxide cathode materials containing multiple transition metals [24]. Elemental distribution mapping has also been used to understand chemical and morphological changes in cathodes after cycling where segregation of transition metals or changes to transition metal density between the surface and bulk of particles can be visualized [25]. When electrodes undergo charge or discharge, state-of-charge (SOC) heterogeneity is also often observed. The local oxidation states of transition metals can deviate from the bulk average and can change the electrochemical characteristics in local regions compared to the bulk. Such heterogeneities are impactful to the operating performance of batteries as they can lead to mechanical degradations, including surface phase changes, crack formation, local overcharging or undercharging, or loss of oxygen from the materials leading to capacity fading or unsafe operating conditions [26]. Battery researchers are interested in studying the formation mechanisms of non-uniform SOC from a practical standpoint. TXM has been used frequently to map charge distribution to evaluate the SOC heterogeneity in lithium-ion battery cathode materials as the high spatial and chemical resolution is needed to probe the local environments within particles [26–29].

TXM has been used for mapping charge distribution in pristine, chemically delithiated, and partially charged or discharged $LiNi_{1-x-y}Mn_xCo_yO_2$ (NMC) materials [30]. Combining XANES analysis with TXM provides bulk sensitive chemical information. Two-dimensional oxidation state mapping of Ni was obtained, which can serve as a proxy for lithium content. This analysis revealed high heterogeneity within both chemically and electrochemically delithiated particles. A gradient in the oxidation state of transition metal on the surface was observed and was found to be more significant in the electrochemically delithiated samples. It was concluded that interactions between the liquid electrolyte and solid electrode present in the electrochemically delithiated sample play a role in facilitating the degradation mechanism of surface reconstruction.

The microstructure can also affect the dynamics of charge distribution. The spatially resolved charge distribution has been investigated in polycrystalline layered oxides prepared with different crystallographic arrangements [31]. NMC materials with radically aligned primary particle grains (rod-NMC) and randomly oriented primary particle grains (gravel-NMC) were studied as model systems. Examining the Ni charge distributions of the particles after slow charging (C/10) using three-dimensional TXM showed variations in the spatial patterns of the Ni valence states between the two-grain orientations (figure 2). To further visualize the charge distributions, two-dimensional nanodomain valence gradient vectors were defined as the local variation of the Ni

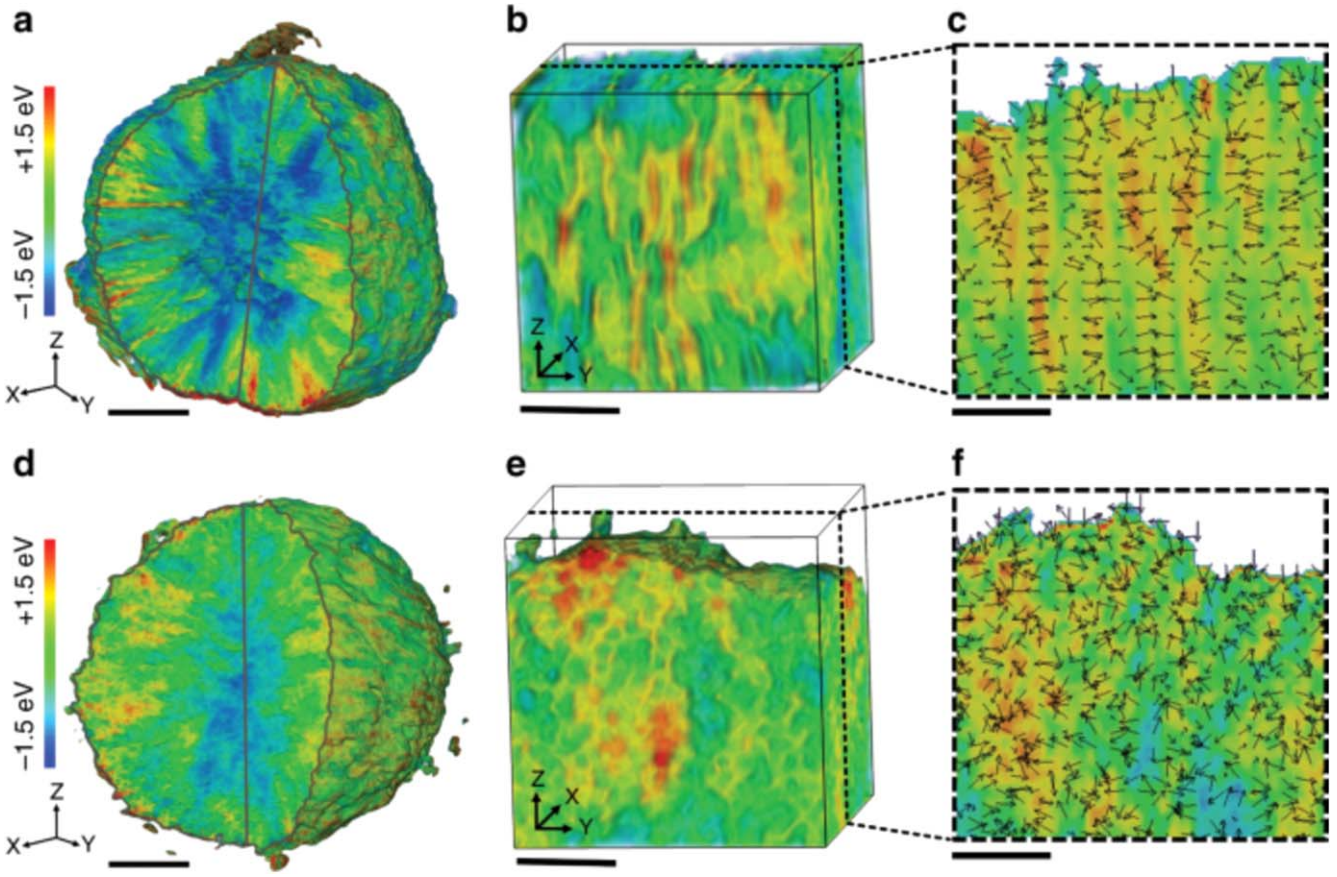

Figure 2. (a) 3D Ni valence state distribution, (b) representative region of the 3D Ni valence state distribution, and (c) 2D nanodomain valence gradient of the rod-NMC. (d) 3D Ni valence state distribution, (e) representative region of the 3D Ni valence state distribution, and (f) 2D nanodomain valence gradient of the gravel-NMC. The nanodomain valence gradient vectors are represented by the black arrows, where the vector direction and magnitude are represented by the arrow direction and arrow length, respectively. The scale bars in (a) and (d) are 3 μm, and the scale bars in (b)–(c) and (e)–(f) are 1 μm. The Ni K-edge absorption energies are color-coded, in which blue stands for lower edge energy and red means higher edge energy. Reproduced with permission from [31]. CC BY 4.0.

absorption edge in three dimensions. The gradient vectors were mostly parallel for the rod-NMCs (figure 2(c)) and randomly oriented for the gravel-NMC (figure 2(f)), suggesting the materials had different redox reaction behaviors guided by the grain crystallographic orientation. Such tailoring of grain orientations can be utilized to guide reaction pathways and charge distribution in electrode materials. Through three-dimensional and two-dimensional TXM analysis, it was concluded that radically aligned grains provided direct lithium ion pathways, improving charge homogeneity and leading to improved capacity retention and suppressed polarization. Understanding and improving charge homogeneity is vital for designing battery materials with increased cycling stability. TXM has been demonstrated to be a useful technique to track and visualize such chemical homogeneities.

In addition to structural and chemical characterizations, TXM techniques can also be used to further elucidate Li^+ transport mechanisms in battery materials. Phase transformations in polycrystalline NMC have been studied [32]. Kuppan *et al* used TXM-XANES to probe the mesoscale delithiation pathways and phase transformation mechanisms at a single-crystal level in octahedral shaped, spinel $Li_xMn_{1.5}Ni_{0.5}O_4$ (LNMO) materials [33]. Probing intrinsic phase transformation behaviors through Ni oxidation state mapping revealed that delithiation of the particles preferentially initiated at the truncated vertices of the octahedral particles, where Li^+ transport has been reported to be more favorable, and then propagated into the bulk (figure 3).

Phase transformations is also an important topic in the research of olivine $LiFeO_4$ (LFO). During Li removal, a phase change occurs that can lead to significant changes in the lattice parameter, increasing strain within particles that can impact conductivity and cycling performance [34]. To examine the mechanism of phase transformation, TXM and STXM combined with mapping of Fe and O K-edges in LFO during chemical delithiation revealed that delithiation occurred more easily at the edges of single-crystal particles [34]. This suggested that morphological defects can kinetically determine the progress of the phase transformation reaction. In a similar study, STXM was used to investigate electrochemically cycled nano-sized LFO particles [35]. Most particles were shown to be either completely lithiated or delithiated at 50% SOC. This study concluded a particle-by-particle mechanism of Li^+ intercalation initiated by the phase change dominated. The sequence of lithiation was also investigated through TXM in partially charged LFO cathodes

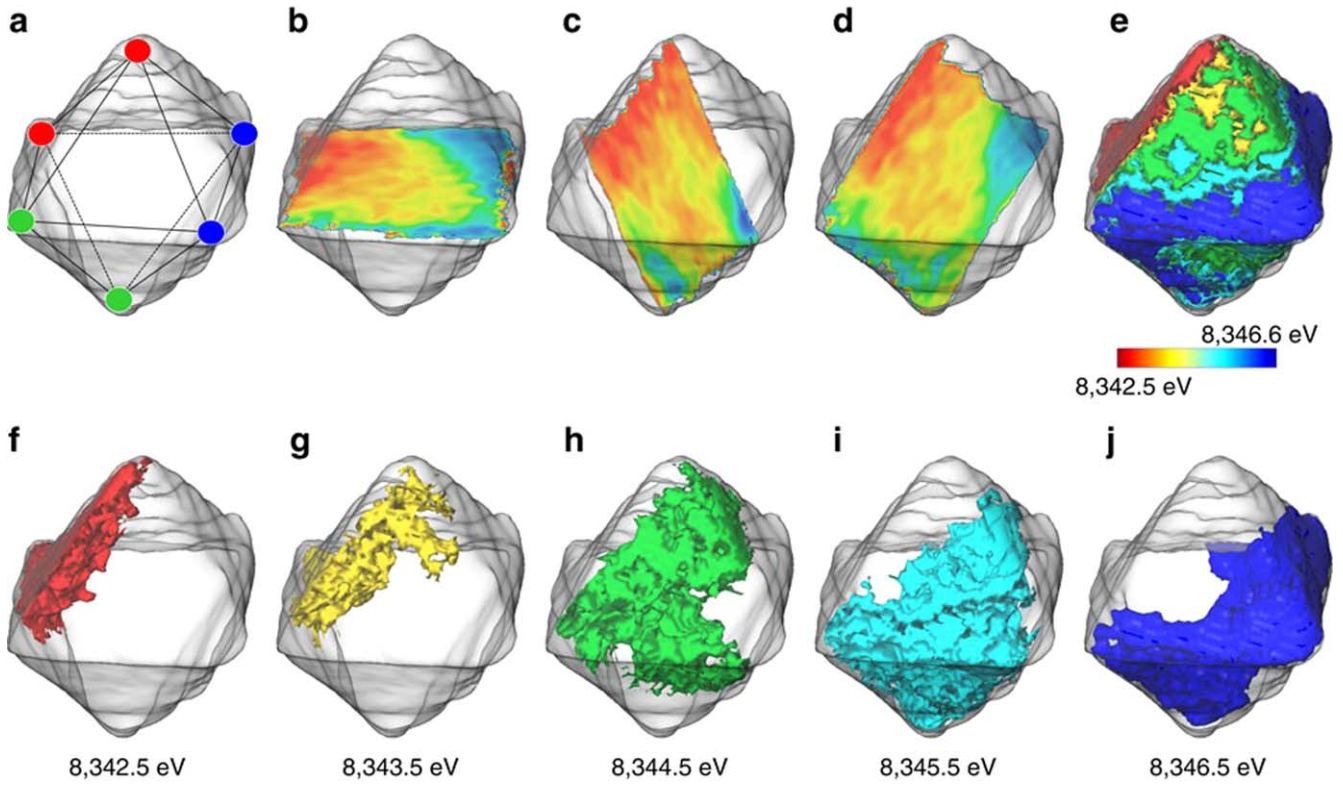

Figure 3. Three-dimensional map of Ni oxidation state at sub-particle scale. The shape of the particle is presented as the transparent grey surface with the internal oxidation state heterogeneity illustrated using the diagonal slices (a)–(d) surfaces of the 3D Ni oxidation state map (e)–(j). All the panels are color-coded in order to show the state of charge heterogeneity at the sub-particle level in a quantitative manner. Reproduced with permission from [33]. CC BY 4.0.

with various microstructures and sizes ranging from 50–500 nm under different electrochemical conditions [28]. Smaller particles were found to lithiate first when electronic conductivity was uniform due to their larger surface area to volume ratio. An *operando* TXM-XANES study tracking the phase transformation processes revealed a rate dependent phase inhomogeneity, where slow rates of charging and discharging lead to more homogenous phase distributions, and fast rates showed coexistence of phases at the multi-particle scale [36]. Two-phase coexistence was also observed for the first time within micron-sized single particles. Such dynamic studies utilizing TXM techniques suggest rate and particle-size dependent mechanisms of Li^+ intercalation in LFO and highlight the importance of rationally designing materials to tailor and optimize particle morphologies.

Phase transformations, lattice volume changes, weakening of grain boundaries, and crack formation caused by mechanical stress induced by anisotropic structural or chemical heterogeneities can all occur during redox reactions in batteries. Such morphological defects and chemomechanical breakdowns can hinder electronic and ionic diffusion pathways leading to capacity fading mechanisms or complete failure of batteries [37, 38]. Mapping these transformations at multiple length and time scales can establish relationships between these processes, identify fading pathways, and provide insights into designing more stable materials. The chemomechanical breakdown of layered NMC was quantified through studying the dependence of crack formation on charging rates [39]. TXM analysis after 50 cycles showed that the crack density increased with the increasing charging rate. Novel mathematical processing of the data allowed for quantification of the porosity and surface area three-dimensional, providing insights into the dynamics of chemo-mechanical degradation.

Three-dimensional TXM was used to study the degradation of NMC particles as materials were cycled to different charge cut-off voltages [40]. XANES mapping of the Ni K-edge for samples with different cycling history combined with nano-resolution x-ray tomography revealed that higher voltage cycling leads to a more rapid decay of capacity and more charge heterogeneity, morphological defects, cracking, and void formation (figure 4). Surface reduction and surface reconstruction were also observed, correlating with charge heterogeneity. Another study combining nanoscale x-ray spectromicroscopy and TXM to study NMC under fast charging conditions revealed a depth-dependent trend of particle fracturing and provided a statistical analysis of chemomechanical transformations to quantify the degradation heterogeneity at multiple length scales fully [41]. *In situ* TXM has also been used to study degradation and SOC heterogeneity in $LiCoO_2$ cycled at different rates [42]. In the study of battery materials, *ex situ*, *in situ,* and *operando* TXM studies have been beneficial in elucidating structural and chemical evolutions as well as providing insights into materials degradations mechanisms at the particle level for both single-crystal and polycrystalline materials.

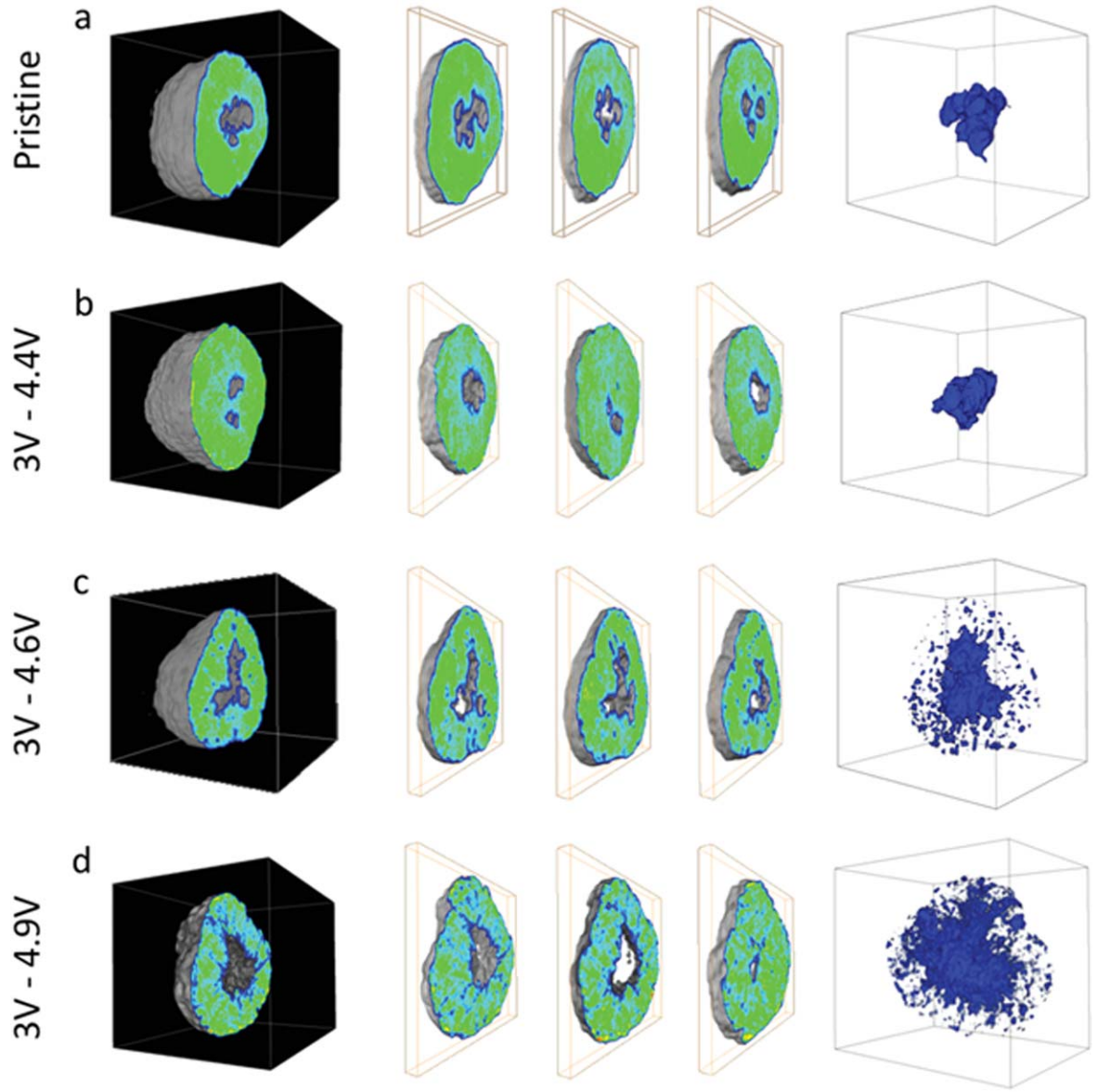

Figure 4. Evolution of the NMC particle morphology upon cycling at C/8 over different voltage windows. (a) Pristine particle, (b) 3.0–4.4 V, (c) 3.0–4.6 V, and (d) 3.0–4.9 V voltage range. The left column is 3D renderings of the secondary particle structure. The middle columns are the virtual slices through different depths of the particle. The right column is the 3D rendering of the void volume (in blue) within the secondary particles. All the particles are about 8–10 microns in diameter. [40] Copyright © 2019, John Wiley and Sons.

Throughout the development of battery research, TXM has been employed as a useful tool to study morphology, chemical distributions, reaction dynamics, and degradation mechanisms in electrode materials. The high resolution provided by synchrotron techniques allows researchers to visualize processes occurring in materials on the nanoscale. However, synchrotron experiments can be sophisticated, *operando* electrochemical cells can be difficult to design, and three-dimensional chemical information can be time consuming to collect and requires large radiation doses that can potentially impact electrolyte or polymer components in the cell [16]. Limited spatial resolution and sample probing depth in the soft x-ray range is a limitation of TXM analysis for mapping of certain elements [30]. However, in combination with other multimodal and multi-length scale characterizations techniques such as transmission electron microscopy, tomography, nano- or micro-diffraction, and ptychograpy, TXM remains a powerful method to visualize and understand chemical properties and reaction dynamics in battery materials. As technologies and data analysis methods continue to advance, TXM methods will have a prosperous future in the study of battery materials.

3. Sample preparations

Compared with electrons, the advantage of x-ray measurements is that they do not require a high vacuum environment because x-rays have less interaction with matter, thus higher penetration power. Especially in hard x-ray experiments, measurements can be done in ambient environments. This

largely simplifies the sample preparations in either *in situ* or *ex situ* experiments.

Nonetheless, the samples for TXM experiments are still subject to certain dimensional requirements. Due to the challenges in the fabrications of FZP, most high-resolution (better than 100 nm) TXMs operate below 15 keV. Furthermore, in XAS mode with TXMs, the measurement energy range is constrained to the vicinity of the specific element's absorption edge, e.g. 8.333 keV for Ni element. The relatively low x-ray energy limits the maximum sample thickness through which measurements with good signal-to-noise ratios (SNR) can be obtained. TXM's depth of focus (DOF) is another factor that limits samples' thickness. If a part of the sample is beyond the DOF, that part of the sample will not be in focus. For good practice, a sample's thickness should always be smaller than the used TXM's DOF. The DOF is x-ray energy dependent. For example, a TXM of 30 nm at 8 keV has a DOF of 23 μm.

In TXM battery experiments, the focus thus far is mainly on the electrode materials. In most experiments, the total sample thickness should be around two absorption lengths, similar to the requirement in a typical bulk XAS experiment in transmission mode [43, 44]. The samples for *ex situ* TXM experiments can be prepared in powders scratched from a cycled electrode or a sharp tip cut out from the electrode, then sealed in thin-wall Kapton® tubes or glass capillaries in a glovebox.

The samples for *in situ* experiments need specially designed functional cells. Reference [2] has a summary of various battery cells for *in situ* x-ray experiments, including that for TXM experiments. The typical battery cells used in TXM experiments are in the forms of coin cell and pouch cell, while various flow cells are also widely used in STXM experiments [45].

Although a high-resolution TXM allows for tens of nanometer resolution characterizations at electrode particle levels, it is important to consider the statistical significance of the measurements. Typically, only a handful of particles are within the FOV and due to sample heterogeneity and, in the case of *in situ* cells, imperfect contact, it is not unusual that different particles within the FOV show different properties, leading to risk of bias in interpretation of the result. Ideally, a large number of measurements of the same type of samples/conditions are needed to avoid bias. With *ex situ* type experiments, this is relatively easy to achieve with a high throughput TXM, e.g. the TXM at FXI beamline of NSLS-II. However, it is not a trivial task for *in situ* type experiments since it is the battery operation conditions rather than the microscope performances determining the throughput of the experiments. Besides, the x-ray radiation may induce side effects to a battery under operating conditions [2, 45–50]. As a rule of thumb, it is necessary to reduce the radiation dose to the cells, which further reduces the *in situ* experiment throughput.

4. Data analysis

TXM data analysis is nontrivial in terms of the amount of data generated (usually on the Terabyte scale) and has relatively poor spectroscopic quality compared with bulk XAS. At tens of nanometer resolution scale, sample drifts due beam-induced heating can be a challenge, especially for 2D or 3D XANES measurements. Analysis usually requires image alignments before the XANES and tomography data processing steps. There is no generic alignment algorithm that can handle the images of various samples in different types of contrast and upon various background features, so careful manual tweaking is needed to get good results.

In the XAS type data analysis, e.g. 2D XANES, the SNR of the spectrum at each individual pixel is low. This is due to the small area of the pixels that are typically under 10^{-2} μm^2. As a comparison, the typical sample area in bulk XAS measurements is larger than 1 mm^2. The small area of the pixels in TXM limits the SNR in each pixel to ~100–300, which corresponds to a pixel count level of 10 000–100 000 and is several orders of magnitude smaller than that in the bulk XAS measurement. On the other hand, the number of pixels in TXM measurements is very large. They are typically composed of more than 1 million spectra in a 2D XANES measurement or more than 1 billion spectra in a 3D XANES measurement with TXM. It is not feasible to fit so many low SNR spectra manually with the conventional XAS analysis approach. Therefore, robust and automatic XAS analysis methods are needed. Whiteline position fitting is one type of XANES spectroscopy analysis method [43, 51, 52] that is widely used in TXM data analysis [53–55]. It is found that the whiteline peak positions of 3d-metals widely used in cathode materials are positively correlated to their oxidation states. Therefore, the whiteline positions of these 3d-metals can be used to track the chemical states of the cathode materials when a battery is cycled to different states of charge. Since the change of the sample absorption in the vicinity of the whiteline position is the largest in the entire spectrum, the signal sensitivity around a whiteline position is highest. However, it should be noted that in certain crystal structures, the absorption peak shape and whiteline position may be strongly affected by factors like the local coordination chemistry and band structures [43, 52]. In such a case, it becomes crucial to carefully calibrate and normalize the spectra so that the edge shift can be used to analyze oxidation states.

There are few available data analysis toolboxes targeted to TXM data analysis [56–58]. One popular package, named TXM-Wizard and developed by Liu and coworkers, has been widely adopted by the TXM community especially for the data collected at the Stanford Synchrotron Radiation Lightsource [56]. However, TXM-Wizard is released only as the compile program so users do not have freedom to contribute further developments. Recently, a Python-based TXM data analysis toolbox with a user-friendly graphic user interface, named TXM_Sandbox, was developed by Xiao *et al* [59]. TXM_Sandbox integrates the tomography reconstruction, 2D XANES, and 3D XANES analysis. The toolbox emphasizes image preprocessing and visualization functions. Automatic image alignments based on a few image registration algorithms are included to handle the alignment tasks with different types of image data. TXM_Sandbox implements

efficient whiteline peak fitting routines based on a multi-process parallelization framework so it can fit a large number of spectra in a short time. The toolbox has carefully designed architecture to guide users to follow the analysis workflow with less ambiguity. In recent years, attempts based on artificial intelligence and machine learning (AI/ML) techniques have been applied in XANES analysis [60–64]. It is demonstrated that AI/ML is capable of finding delicate correlations between different parameters hidden in a large amount of data from XANES spectra with TXM [40, 65, 66]. TXM_Sandbox also includes user interfaces to few AI/ML routines out of Scikit-Learn [67].

5. Discussions and outlooks

Due to the limited surface sensitivity and SNR in the measurements, TXM is not a surface-sensitive technique. It is a powerful tool in providing structural and performance information at mesoscales. However, in complex systems like lithium-ion batteries, components of different length scales all matter in the overall performance of the system. Not a single technique can provide complete information for thoroughly understanding the system. It is necessary to combine different techniques, including various x-ray techniques, electron microscopy techniques, and electrochemical characterization techniques, to obtain complementary information. Although the multimodal characterization approach becomes almost a standard in battery materials research, the field still mostly lacks quantitative and correlative data analysis of different kinds of data. Specific AI/ML applications demonstrated the strength in handling high-dimensional complex data, yet there are no obvious solutions to quantitative and correlative data analysis regarding battery materials.

One hurdle in the current approach is data representativeness. It is not feasible to obtain statistically significant representative data at every level with the different techniques. One possible solution is to use certain high-throughput techniques to guide and correlate results from low-throughput techniques that have limited data. For instance, TXM, like the one at NSLS-II, is capable of high-throughput measurements. It is possible to utilize TXM to select representative sample groups for further characterizations with other low-throughput microscopic techniques.

As new technology emerges, TXM will continue to develop as a tool to study the morphology and chemical composition in novel and diverse electrode materials. Improvements and streamlining of software for data processing are already in development, a topic which we have previously touched on. Tools to integrate TXM data processing and data from additional techniques will likely emerge in the near future and would allow for efficient multimodal analysis at a variety of length and time scales. If the issue of beam damage can be mitigated or solved, TXM experiments can be widely applied to a variety of battery systems and materials with minimal limitations. Ultimately, the advancement of TXM, in tandem with other characterization techniques, will prove to be a vital asset for battery materials research and development in the future.

Acknowledgments

This research used resources of the beamline FXI/18ID of the National Synchrotron Light Source II, a U.S. Department of Energy (DOE) Office of Science User Facility operated for the DOE Office of Science by Brookhaven National Laboratory under Contract No. DE-SC0012704. The work at Virginia Tech was supported by the National Science Foundation under contract DMR 1832613.

Data availability statement

No new data were created or analysed in this study.

ORCID iDs

Stephanie Spence https://orcid.org/0000-0002-7039-3554
Xianghui Xiao https://orcid.org/0000-0002-7142-3452

References

[1] Lin F *et al* 2017 Synchrotron x-ray analytical techniques for studying materials electrochemistry in rechargeable batteries *Chem. Rev.* **117** 13123–86
[2] Bak S M, Shadike Z, Lin R, Yu X and Yang X Q 2018 *In situ*/operando synchrotron-based x-ray techniques for lithium-ion battery research *NPG Asia Mater.* **10** 563–80
[3] Wen H, Cherukara M J and Holt M V 2019 Time-resolved x-ray microscopy for materials science *Annu. Rev. Mater. Res.* **49** 389–415
[4] Cao C, Toney M F, Sham T K, Harder R, Shearing P R, Xiao X and Wang J 2020 Emerging x-ray imaging technologies for energy materials *Mater. Today* **34** 132–47
[5] Kirz J and Jacobsen C 2009 The history and future of x-ray microscopy *J. Phys. Conf. Ser.* **186** 012001
[6] Kaulich B, Thibault P, Gianoncelli A and Kiskinova M 2011 Transmission and emission x-ray microscopy: operation modes, contrast mechanisms and applications *J. Phys. Condens. Matter* **23** 083002
[7] Guttmann P and Bittencourt C 2015 Overview of nanoscale NEXAFS performed with soft x-ray microscopes *Beilstein J. Nanotechnol.* **6** 595–604
[8] Yoon T H 2009 Applications of soft x-ray spectromicroscopy in material and environmental sciences *Appl. Spectrosc. Rev.* **44** 91–122
[9] Michette G A 1986 *Optical Systems for Soft X-rays* (New York: Plenum)
[10] Attwood D 1999 *Soft X-rays and Extreme Ultraviolet Radiation: Principles and Applications* (Cambridge: Cambridge University Press)
[11] Howells H, Jacobsen C and Warwick A 2006 *Principles and Applications of Zone Plate X-ray Microscopes* (Berlin: Springer)
[12] Howells M R *et al* 2009 An assessment of the resolution limitation due to radiation-damage in x-ray diffraction microscopy *J. Electron Spectrosc. Relat. Phenom.* **170** 4–12

[13] Huang X, Miao H, Steinbrener J, Nelson J, Shapiro D, Stewart A, Turner J and Jacobsen C 2009 Signal-to-noise and radiation exposure considerations in conventional and diffraction x-ray microscopy *Opt. Express* **17** 13541

[14] Ge M, Coburn D S, Nazaretski E, Xu W, Gofron K, Xu H, Yin Z and Lee W K 2018 One-minute nano-tomography using hard x-ray full-field transmission microscope *Appl. Phys. Lett.* **113** 083109

[15] Whittingham M S 2004 Lithium batteries and cathode materials *Chem. Rev.* **104** 4271–302

[16] Nelson Weker J and Toney M F 2015 Emerging *in situ* and operando nanoscale x-ray imaging techniques for energy storage materials *Adv. Funct. Mater.* **25** 1622–37

[17] Pietsch P and Wood V 2017 X-ray tomography for lithium ion battery research: a practical guide *Annu. Rev. Mater. Res.* **47** 451–79

[18] Cooper S J *et al* 2014 Image based modelling of microstructural heterogeneity in $LiFePO_4$ electrodes for Li-ion batteries *J. Power Sources* **247** 1033–9

[19] Zhu Z *et al* 2020 Gradient-morph $LiCoO_2$ single crystals with stabilized energy density above 3400 W h L -1 *Energy Environ. Sci.* **13** 1865–78

[20] Lin C-H *et al* 2020 Systems-level investigation of aqueous batteries for understanding the benefit of water-in-salt electrolyte by synchrotron nanoimaging *Sci. Adv.* **6** eaay7129

[21] Zhang F *et al* 2020 Surface regulation enables high stability of single-crystal lithium-ion cathodes at high voltage *Nat. Commun.* **11** 3050

[22] Lou S *et al* 2020 Insights into interfacial effect and local lithium-ion transport in polycrystalline cathodes of solid-state batteries *Nat. Commun.* **11** 5700

[23] Liu Y, Meirer F, Wang J, Requena G, Williams P, Nelson J, Mehta A, Andrews J C and Pianetta P 2012 3D elemental sensitive imaging using transmission x-ray microscopy *Anal. Bioanal. Chem.* **404** 1297–301

[24] Rahman M M *et al* 2019 Surface characterization of li-substituted compositionally heterogeneous $NaLi0.045Cu0.185Fe0.265Mn0.505O_2$ sodium-ion cathode material *J. Phys. Chem.* C **123** 11428–35

[25] Yang F, Liu Y, Martha S K, Wu Z, Andrews J C, Ice G E, Pianetta P and Nanda J 2014 Nanoscale morphological and chemical changes of high voltage lithium-manganese rich NMC composite cathodes with cycling *Nano Lett.* **14** 4334–41

[26] Nanda J, Remillard J, O'Neill A, Bernardi D, Ro T, Nietering K E, Go J-Y and Miller T J 2011 Local state-of-charge mapping of lithium-ion battery electrodes *Adv. Funct. Mater.* **21** 3282–90

[27] Gent W E *et al* 2016 Persistent state-of-charge heterogeneity in relaxed, partially charged $Li_{1-x}Ni_{1/3}Co_{1/3}Mn_{1/3}O_2$ secondary particles *Adv. Mater.* **28** 6631–8

[28] Li Y *et al* 2015 Effects of particle size, electronic connectivity, and incoherent nanoscale domains on the sequence of lithiation in $LiFePO_4$ porous electrodes *Adv. Mater.* **27** 6591–7

[29] Wei C, Xia S, Huang H, Mao Y, Pianetta P and Liu Y 2018 Mesoscale battery science: the behavior of electrode particles caught on a multispectral x-ray camera *Acc. Chem. Res.* **51** 2484–92

[30] Tian C, Xu Y, Nordlund D, Sun Z, Liu Y, Doeff M, Lin F and Liu J 2017 Charge heterogeneity and surface chemistry in polycrystalline cathode materials highlights delithiated samples show state-of-charge heterogeneity surface reconstruction is less apparent in chemically delithiated samples electrolytic solution plays a vita *Joule* **2** 1–14

[31] Xu Z *et al* 2020 Charge distribution guided by grain crystallographic orientations in polycrystalline battery materials *Nat. Commun.* **11** 83

[32] Mu L, Yuan Q, Tian C, Wei C, Zhang K, Liu J, Pianetta P, Doeff M M, Liu Y and Lin F 2018 Propagation topography of redox phase transformations in heterogeneous layered oxide cathode materials *Nat. Commun.* **9** 2810

[33] Kuppan S, Xu Y, Liu Y and Chen G 2017 Phase transformation mechanism in lithium manganese nickel oxide revealed by single-crystal hard x-ray microscopy *Nat. Commun.* **8** 14309

[34] Boesenberg U *et al* 2013 Mesoscale phase distribution in single particles of $LiFePO_4$ following lithium deintercalation *Chem. Mater.* **25** 1664–72

[35] Chueh W C, El Gabaly F, Sugar J D, Bartelt N C, McDaniel A H, Fenton K R, Zavadil K R, Tyliszczak T, Lai W and McCarty K F 2013 Intercalation pathway in many-particle $LiFePO_4$ electrode revealed by nanoscale state-of-charge mapping *Nano Lett.* **13** 866–72

[36] Wang J, Chen-Wiegart Y C K and Wang J 2014 In operando tracking phase transformation evolution of lithium iron phosphate with hard x-ray microscopy *Nat. Commun.* **5** 4570

[37] Xu Z, Rahman M M, Mu L, Liu Y and Lin F 2018 Chemomechanical behaviors of layered cathode materials in alkali metal ion batteries *J. Mater. Chem.* A **6** 21859–84

[38] Mu L *et al* 2018 Oxygen release induced chemomechanical breakdown of layered cathode materials *Nano Lett.* **18** 3241–9

[39] Xia S *et al* 2018 Chemomechanical interplay of layered cathode materials undergoing fast charging in lithium batteries *Nano Energy* **53** 753–62

[40] Mao Y *et al* 2019 High-voltage charging-induced strain, heterogeneity, and micro-cracks in secondary particles of a nickel-rich layered cathode material *Adv. Funct. Mater.* **29** 1–11

[41] Yang Y *et al* 2019 Quantification of heterogeneous degradation in Li-ion batteries *Adv. Energy Mater.* **9** 1900674

[42] Xu Y *et al* 2017 *In situ* visualization of state-of-charge heterogeneity within a $LiCoO_2$ particle that evolves upon cycling at different rates *ACS Energy Lett.* **2** 1240–5

[43] Newville M 2014 *Reviews in Mineralogy and Geochemistry* **78** 33–74 Fundamentals of XAFS

[44] Gaur A and Shrivastava B D 2015 Speciation using x-ray absorption fine structure (XAFS) *Rev. J. Chem.* **5** 361–98

[45] Smith J W and Saykally R J 2017 Soft x-ray absorption spectroscopy of liquids and solutions *Chem. Rev.* **117** 13909–34

[46] Wolf M, May B M and Cabana J 2017 Visualization of electrochemical reactions in battery materials with x-ray microscopy and mapping *Chem. Mater.* **29** 3347–62

[47] Wang J, Morin C, Li L, Hitchcock A P, Scholl A and Doran A 2009 Radiation damage in soft x-ray microscopy *J. Electron Spectrosc. Relat. Phenom.* **170** 25–36

[48] Lim C, Kang H, De Andrade V, De Carlo F and Zhu L 2017 Hard x-ray-induced damage on carbon-binder matrix for *in situ* synchrotron transmission x-ray microscopy tomography of Li-ion batteries *J. Synchrotron Radiat.* **24** 695–8

[49] Cazaux J 1997 A physical approach to the radiation damage mechanisms induced by x-rays in x-ray microscopy and related techniques *J. Microsc.* **188** 106–24

[50] Nelson J, Yang Y, Misra S, Andrews J C, Cui Y and Toney M F 2013 Identifying and managing radiation damage during *in situ* transmission x-ray microscopy of Li-ion batteries *Proceedings of SPIE* 8851, 88510B

[51] Bunker G Interpreting XANES (http://gbxafs.iit.edu/training/XANES_intro.pdf)

[52] Henderson G S, De Groot F M F and Moulton B J A 2014 X-ray absorption near-edge structure (XANES) spectroscopy *Rev. Mineral. Geochem.* **78** 75–138

[53] Boesenberg U *et al* 2013 Mesoscale phase distribution in single particles of $LiFePO_4$ following lithium deintercalation *Chem. Mater.* **25** 1664–72
[54] Kuppan S, Xu Y, Liu Y and Chen G 2017 Phase transformation mechanism in lithium manganese nickel oxide revealed by single-crystal hard x-ray microscopy *Nat. Commun.* **8** 1–10
[55] Mu L, Yuan Q, Tian C, Wei C, Zhang K, Liu J, Pianetta P, Doeff M M, Liu Y and Lin F 2018 Propagation topography of redox phase transformations in heterogeneous layered oxide cathode materials *Nat. Commun.* **9** 2810
[56] Liu Y, Meirer F, Williams P A, Wang J, Andrews J C and Pianetta P 2012 TXM-Wizard: a program for advanced data collection and evaluation in full-field transmission x-ray microscopy *J. Synchrotron Radiat.* **19** 281–7
[57] Ge M and Lee W K 2020 PyXAS-an open-source package for 2D x-ray near-edge spectroscopy analysis *J. Synchrotron Radiat.* **27** 567–75
[58] Lerotic M, Mak R, Wirick S, Meirer F and Jacobsen C 2014 Mantis: a program for the analysis of x-ray spectromicroscopy data *J. Synchrotron Radiat.* **21** 1206–12
[59] Xiao X, Xu Z, Lee W K and Lin F 2021 TXM_Sandbox-An Integrated Transmission X-ray Microscopy Data Analysis Package with Graphic User Interface Based on Jupyter, to be Submitted
[60] Erdem Günay M and Yıldırım R 2020 Recent advances in knowledge discovery for heterogeneous catalysis using machine learning *Catal. Rev.-Sci. Eng.* **63** 120–64
[61] Guda A A *et al* 2019 Quantitative structural determination of active sites from *in situ* and operando XANES spectra: from standard *ab initio* simulations to chemometric and machine learning approaches *Catal. Today* **336** 3–21
[62] Mizoguchi T and Kiyohara S 2020 Machine learning approaches for ELNES/XANES *Microscopy* **69** 92–109
[63] Carbone M R, Yoo S, Topsakal M and Lu D 2019 Classification of local chemical environments from x-ray absorption spectra using supervised machine learning *Phys. Rev. Mater.* **3** 33604
[64] Zheng C *et al* 2017 Automated generation and ensemble-learned matching of x-ray absorption spectra *npj Comput. Mater.* **4** 12
[65] Duan X, Yang F, Antono E, Yang W, Pianetta P, Ermon S, Mehta A and Liu Y 2016 Unsupervised data mining in nanoscale x-ray spectro-microscopic study of NdFeB magnet *Sci. Rep.* **6** 34406
[66] Zhang K *et al* 2017 Finding a needle in the haystack: identification of functionally important minority phases in an operating battery *Nano Lett.* **17** 7782–8
[67] Pedregosa F *et al* 2011 Scikit-learn: Machine Learning in Python *J. Machine Learning Res.* **12** 2825–30